Annals of Hepatology
The Official Journal of the Mexican Association of Hepatology, the Latin-American Association for Study of the Liver and the Canadian Association for the Study of the Liver

ORIGINAL ARTICLE

July-August, Vol. 17 No. 4, 2018: 645-654

Rapamycin Combi with TAE on the Growth, Metastasis, and Prognosis of Hepatocellular Carcinoma in Rat Models

Hong-Wei Lei,*,*** Jie Cai,*,*** Cheng-Ming Li,*,*** Fang Yang,*,*** Wan-Qing Shi,*,*** Li-Ping Wang,*,*** You-Ying Feng**,***

* Department of Interventional Radiology, the First People's Hospital of Jingzhou, Jingzhou, Hubei, P.R. China
** Department of Central Sterile Supply, the First People's Hospital of Jingzhou, Jingzhou, Hubei, P.R. China
*** First Hospital affiliated to Yangtze University, Jingzhou, Hubei Province, China.

ABSTRACT

Introduction and aim. To investigate the effect of mTOR inhibitor Rapamycin combined with transcatheter arterial embolization (TAE) on the growth, metastasis, and prognosis of hepatocellular carcinoma (HCC) in rat model. **Material and method.** McA-RH7777 cells were used to construct rat models of HCC, which were randomly divided into Model, Rapamycin, TAE, and Rapamycin + TAE groups. Quantitative reverse transcription-PCR (qRT-PCR) and Western Blot were used to detect the expression of Epithelial-Mesenchymal Transition (EMT)-related molecules, and immunohistochemical staining to determine the expression of EMT-related proteins, angiogenic factors as well as microvessel density (MVD)-CD34. **Results.** The hepatic tumor volume of rats in the other three groups were all significantly smaller than the Model group on the 7th, 14th, and 21st day after treatment and the combination treatment was apparently more effective than either treatment alone. Besides, both the number and the size of metastatic nodules of HCC rats after combination treatment were remarkably reduced. In addition, compared with rats in the Rapamycin + TAE group, N-cadherin, Vimentin, HIF-1α, VEGF, and MVD-CD34 were obviously enhanced, while E-cadherin was lowered in those TAE group, which were the complete opposite to the Rapamycin group. Besides, the median survival time of rats in the Rapamycin + TAE group was evidently longer than the resting groups. **Conclusion.** Rapamycin combined with TAE may effectively suppress the EMT formation and angiogenesis, thereby inhibiting the growth and lung metastasis of HCC rats, which provides a new idea for countering the recurrence and metastasis of HCC.

Key words. Combination therapy. mTOR. Tumor volume. EMT.

INTRODUCTION

Hepatocellular carcinoma (HCC) ranks the sixth most common fatal tumor in the human liver and the second leading cause of cancer-related death in the world, with an estimated diagnosis of more than 800,000 new patients each year.[1,2] In clinical trials, transcatheter arterial embolization (TAE) has been widely used for those HCC patients who could not receive surgery, with the characteristics of precisely targeted, minimally invasive, as well as repeatable and well-tolerated.[3,4] Nevertheless, the incomplete embolization or tumor angiogenesis owing to the TAE was revealed by a great body of studies to lead to tumor recurrence and metastasis.[5-7] In recent years, some combination therapies of TAE with some anti-angiogenic methods have presented preferable therapeutic effect. For example, in the study by Nitta-Seko A, *et al*., thalidomide in combination with TAE can effectively promote the anti-tumor effect in rabbits with VX2 hepatic tumor.[8] But the efficacy in a considerable number of patients with HCC is still not clear, especially for those HCC patients with metastasis and recurrence.[9] In this regard, it is of great importance to further identify the optimal therapy to improve the survival of advanced HCC.

Mammalian Target of Rapamycin (mTOR) is an atypical highly conserved serine/threonine protein kinase implicated in the regulation of many cellular activities, such as growth, proliferation, cell cycles and metabolism, as well as mediating tumor angiogenesis.[10] A large number of studies have discovered the inappropriate mTOR activa-

Manuscript received: September 04, 2017. **Manuscript accepted:** October 17, 2017.

DOI: 10.5604/01.3001.0012.0948

tion in various malignancies, including lung cancer, ovarian cancer, and HCC.[11,12] Thus, inhibitors of mTOR pathway have become standard anti-tumor strategies, especially in HCC. As reported by Zhao Q, *et al*., Aspirin may exert inhibitory effects on tumor angiogenesis through blocking the expressions of mTOR signaling pathway-related factors in murine HCC and sarcoma models.[13] Besides, Xue ZG and his group identified Cardamonin as a novel angiogenesis inhibitor with respect to ovarian cancer treatment, partially linked to the inhibition of the mTOR of Rapamycin.[14] Rapamycin, as one of the best-known inhibitor of mTOR, is a new type of highly effective immunosuppressive agent, which can inhibit the protein kinase catalytic activity of mTOR,[15] further suppressing angiogenesis to inhibit the growth and metastasis of many malignant tumor cells.[16,17] Current knowledge suggests that the activity of mTOR depends on its combination with other molecules to form two functionally distinct multiprotein complexes, namely mTORC1 (mTOR complex 1) and mTORC2 (mTOR complex 2).[18] In combination with FKBP12, Rapamycin could selectively inhibit the activity of mTORC1 via association with its intracellular receptor FK-506 binding protein 12 (FKBP12), but not mTORC2.[19] As such, we would only investigate the mTORC1 and refer to it as mTOR in this study. Of note, in responding patients, the developing of Rapamycin resistance would restrict the overall clinical benefit, and combination therapy has become a promising method to improve the efficacy of rapamycin.[20]

However, it has not been elucidated whether Rapamycin combined with TAE has a synergistic anti-tumor effect. In light of the uncertainties, this study constructed the rat model of HCC by using McA-RH7777 cells to explore the impact of Rapamycin combined with TAE on the growth, metastasis, and prognosis of HCC in rat model.

MATERIAL AND METHODS

Ethics statement

The design of the animal experiments was approved by the Ethics Committee of the First People's Hospital of Jingzhou for Laboratory Animals, and all the research behaviors conducted in the study were strictly in accordance with the regulations for the care and use of laboratory animals by the International Association for the Study Pain (IASP).[21]

Animals

The clean grade Buffalo rats selected were 6~8 weeks old with the weight 160~180 g, half male and half female (purchased from Shanghai SLAC Laboratory Animal Co. Ltd., Shanghai, People's Republic of China), and were housed in clean grade animal room with unrestricted access to food and water in a room temperature maintained at 22~25 °C, with normal circadian rhythm as well as routine food and water supply.

Establishment of HCC tumor-bearing rats models

The McA-RH7777 rat hepatoma cell line (purchased from the ATCC (American Type Culture Collection, CRL-1601) in the USA) were cultured with high-glucose DMEM (Dulbecco's modified Eagle's medium) (Hyclone, USA) containing 10% fetal bovine serum (FBS) (Gibco, USA) in a 37 °C incubator with 5% CO_2. When covered culture flasks, cells were digested with trypsin and centrifuged for 5 min at 1000 rpm. After re-suspended, the cell density was adjusted to 4×10^6/mL. Rats were injected subcutaneously into the thigh with 0.5 mL cell suspension for tumor-bearing. The subcutaneous tumor mass was measured regularly with vernier calipers. Two weeks later, the subcutaneous tumor was obtained for liver tumor transplantation. Rats were anesthetized with 10% chloral hydrate solution (0.3 mL/100 g of body weight, Jiangsu Hengrui Medicine Co, Ltd, Jiangsu, China), and the subcutaneous tumor was cut and collected, which was preserved in ice-cold normal saline. After removed the tumor capsule and necrotic tissues of the specimens, the remaining tumor tissues were cut into cubes with 2 mm^3 in size. After that, the abdominal wall of the rats was opened to expose the liver, and the left lobe of the liver was gently put aside for fixing, and the ophthalmic forceps pierced the hepatic capsular and deliver the HCC tumor block to a depth of about 0.5 cm. Then, the abdominal wall was closed before the rats were sent to animal center.

Grouping

All rats were intraperitoneally anesthetized for MRI scanning to observe the tumor formation 14 days after implantation. Then, forty successfully-established model rats were selected and randomly divided into four groups: Model group, Rapamycin group, TAE group, and Rapamycin + TAE group, with 10 rats in each group. The rats were given general anesthesia before a midline abdominal incision. Next, under the operating microscope (Zeiss OPMI 6-S, Aalen, Germany), a silicone catheter (outer diameter 0.8 mm) with a tip in the shape of a hockey-stick was inserted retrogradely into the left hepatic artery by way of the gastroduodenal artery. After that, the catheter was firmly fixed for hepatic arterial infusion, with 0.5 mL/kg of lipiodol in the TAE and the Rapamycin + TAE groups, or with the same volume of saline in the Model and the

Rapamycin groups. Next, the catheter was removed, the gastroduodenal artery was ligated, and the incision was closed in two layers. Three days after the operation, rats in the Rapamycin group and the Rapamycin + TAE group were intraperitoneally injected with mTOR inhibitor Rapamycin (S1039, Pfizer) once a day and 4 mg/kg each time. After 5 days of continuous administration, Rapamycin was changed to 3 times a week before withdrawal 2 weeks after the operation. At the same time, rats in the Model and the TAE groups were intraperitoneally injected with equal dose of normal saline. MRI examination was performed every 7 days after operation. The groupings and interventions of experimental procedures were shown in figure 1.

Lung metastatic nodules

Thirty-one days after operation (two weeks after treatment), 5 rats were randomly selected from each group and killed under the anesthesia with 10% chloral hydrate. Lung samples were obtained to observe the lung metastasis. The quantitative analysis of lung metastatic nodules was carried out according to the method reported in a previous study.[22] The counting of lesions depends on a light microscope and the total area of lung tissues in each rat was measured by using an image analyzer (VIP-21C, Olympus-Ikegami Tsushin Co., Tokyo).

qRT-PCR

The extraction of total RNA was operated in line with the instructions on the Trizol reagent (Invitrogen Life Technologies, Carlsbad, CA, USA), and the RNA extract was determined for its purity and concentration by a NanoDrop2000 spectrophotometer (Thermo Scientific, Willmington, DE, USA). The primer sequences for PCR were designed by using Primer 5.0 software based on the gene sequences published in the Genbank and were synthesized by Sangon Biotech (Shanghai) Co. Ltd (Table 1). The PCR reaction system was prepared according to instructions on the ABI PRISM 7500 real-time PCR System (ABI). And the conditions for real-time PCR were as follows: pre-denaturation for 10 s at 95 °C and 40 cycles of 5 s at 94 °C, 5 s at 60 °C, and 10 s at 72 °C. With GAPDH as the internal reference gene, each gene of each sample had 3 replicates and the dissolution curve was used to evaluate the reliability of PCR. CT value (the inflection point of

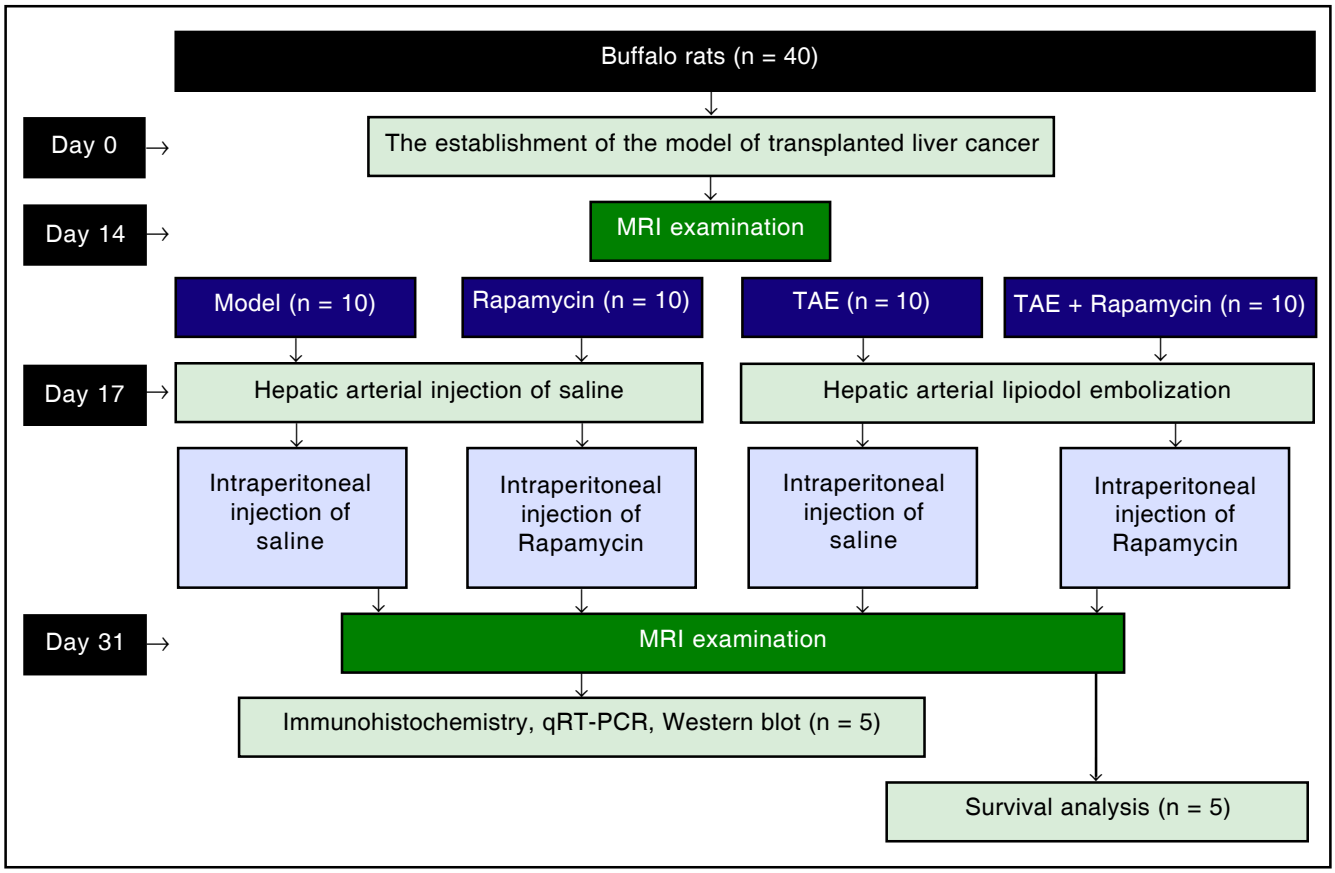

Figure 1. *Flow chart illustrating a process of gouping.*

Table 1. List of primer sequences used in qRT-PCR experiments.

Gene	Primer sequences (i5' – 3')
E-cadherin	F: GCCCTGCCAATCCCGATGAAA R: GGGGTCAGTATCAGCCGCT
N- cadherin	F: GCGTCTGTAGAGGCTTCTGG R: GCCACTTGCCACTTTTCCTG
Vimentin	F: GCTTCAGAGAGAGGAAGCCGAAAA R: CCGTGAGGTCAGGCTTGGAAA
GAPDH	F: GGGGAGCCAAAAGGGTCATCATCT R: GACGCCTGCTTCACCACCTTCTTG

the amplification curve) was read to calculate the relative expression level of target genes according to 2-ΔΔCt:

$$\Delta Ct = CT_{(target\ gene)} - CT_{(internal\ reference\ gene),}$$

$$\Delta\Delta Ct = \Delta Ct_{(experiment\ group)} - \Delta Ct_{(control\ group).}$$

The experiment was repeated 3 times.

Western blot

The total protein was determined for concentration according to the instructions on BCA Kit (Wuhan Boster Biological Technology, LTD, China). The protein samples were added with loading buffer, boiled for 10 min at 95 °C, and loaded with 40 ug/well. The protein was isolated by with 10% SDS-polyacrylamide gel electrophoresis (Wuhan Boster Biological Technology, LTD, China), with voltage from 80 V for concentrated gel to 120 V for separating gel. Proteins after electrophoretic separation were transferred to polyvinylidene fluoride (PVDF) membrane for 90~120 min with the constant voltage 100 mV. The 5% skim milk-PBS solution was blocked for 1 h at room temperature with primary antibodies E-cadherin (ab1416, 1/100), N-cadherin (ab18203, 1 μg/mL), Vimentin (ab8978, 1/1000) and β-actin (ab8226, 1 μg/mL), which were all purchased from Abcam (Cambridge, MA, USA). The membrane was washed 3 times with Tris Buffered Saline, with Tween (TBST) buffer for 5 min and cultured for 1 h at room temperature with secondary antibodies. Then, the membrane was washed with TBST buffer for 5 min for another 3 times and developed by a chemiluminescence (ECL) reagent (Thermo Scientific Pierce, Rockford, IL, USA). The internal reference gene was β-actin and the experiment was repeated three times.

Immunohistochemical staining

HCC tissues (3-mm-thick slices) were fixed in 10% formalin solution and embedded with paraffin to make 4 μm tissue sections. The sections were baked and soaked in xylene solution for 10 min, dewaxed with gradient alcohol for 5 min, washed with water before incubation in 3% H_2O_2 for 10 min at 37 °C, blocked with serum for 30 min, and washed with PBS for 5 min × 3 times before overnight reaction at 4 °C with primary antibodies: E-cadherin (ab1416, 1/50), N-cadherin (ab18203, 1 μg/mL), Vimentin (ab8978, 1 μg/mL), VEGF (ab53465, 1/500), HIF-1α (ab113642, 1/500) (all purchased from Abcam, Cambridge, MA, USA). Biotinylated secondary antibodies were then added to incubate for 30 min at 37 °C. Sections were washed 3 times with PBS buffer, incubated for 30 min with immune complexes at 37 °C, developed with diaminobenzidine (DAB) for 20 min, and terminated with PBS buffer. Sections were dehydrated with conventional ethanol, transparentized with xylene, and mounted with neutral resin. Four visual fields randomly selected in each section under an optical microscope (Olympus Optical Co., Tokyo, Japan) were taken for photos to observe the expression of positive cells. The experiment was repeated three times.

MVD Determination

The determination of MVD-CD34 was performed in line with the method described by Zhang Q, *et al*.[23] The stained sections were screened at low power field (×40) to select 5 hot spots, that is, areas with the most the most intense neovascularization. The counting of micro-vessel in hot spots was conducted at high power field (×200). Any brown-stained endothelial cell or cell cluster, which can be clearly separated from adjacent micro-vessels, tumor cells, and other connective-tissue elements, was counted as one micro-vessel, regardless of the existence of a vessel lumen. The mean value of the micro-vessel number of the five hot spots was taken as the MVD, which was presented by the absolute number of micro-vessels per 0.74 mm^2 (×200).

Survival observation

The remaining 5 rats in each group were observed for general conditions and date of death of each rat was recorded. The standard date of death should be subjected to natural death or killed on the verge of death. The survival period of rats was calculated, including the date of inoculation and the day of death, and the median survival period was also calculated.

Statistical method

All data were processed by the means of statistical analysis software SPSS 21.0 (SPSS, Inc, Chicago, IL, USA). The

measurement data were presented by mean ± standard deviation, and the comparison among multiple groups was conducted by One-Way ANOVA, while comparison between two groups was analyzed by t-test. Survival analysis was performed by Kaplan-Meier method. $P < 0.05$ means the difference with statistical significance.

RESULTS

Establishment of HCC rat models

The rate of tumor formation was 100% for orthotopic hepatic transplantation. On the 1st day after operation, the rats showed a depression-like state with decreased foraging activities, which all disappeared on the 3rd day, and rats were in good conditions without any other complications or death. On the 14th day after tumor transplantation, MRI examination showed visible hepatic tumor in all the 40 rats, which was round or slightly oval in shape and characterized by expansive growth with low signal intensity on T1WI and high signal intensity on T2W1. Small patchy necrosis with uneven signal intensity can be seen in the middle of lesions, and envelope signal was visible on the edge of tumors, showing clear boundary with surrounding normal hepatic parenchyma (Figure 2A-2B). Rats in the Model, Rapamycin, TAE, and Rapamycin + TAE groups showed no statistical difference in the average volume of hepatic tumor (Figure 2C).

Comparison of tumor volume of rats among different groups after the combination treatment with Rapamycin and TAE

On the 7th and 14th day after treatment, the tumor volume of rats in the Rapamycin, TAE and Rapamycin + TAE groups was appreciably smaller than that of the Model group; and the Rapamycin + TAE group was also apparently smaller than either treatment alone (all $P < 0.05$). Further, the difference was more pronounced after 21 days treatment. However, there was no significant difference between the Rapamycin group and the TAE group ($P > 0.05$) (Figure 3).

Effect of the combination treatment with Rapamycin and TAE on lung metastasis of rats

On the 31st day after operation (2 weeks after treatment), the lung metastasis rate of rats was 60% (3/5, Model), 40% (2/5, Rapamycin), 100% (5/5, TAE), and 60% (3/5, Rapamycin + TAE), respectively. Meanwhile, concerning the number, as well as the size of metastatic nodules, rats in the TAE group were remarkably higher than the other three groups, while the Rapamycin group was significan lower

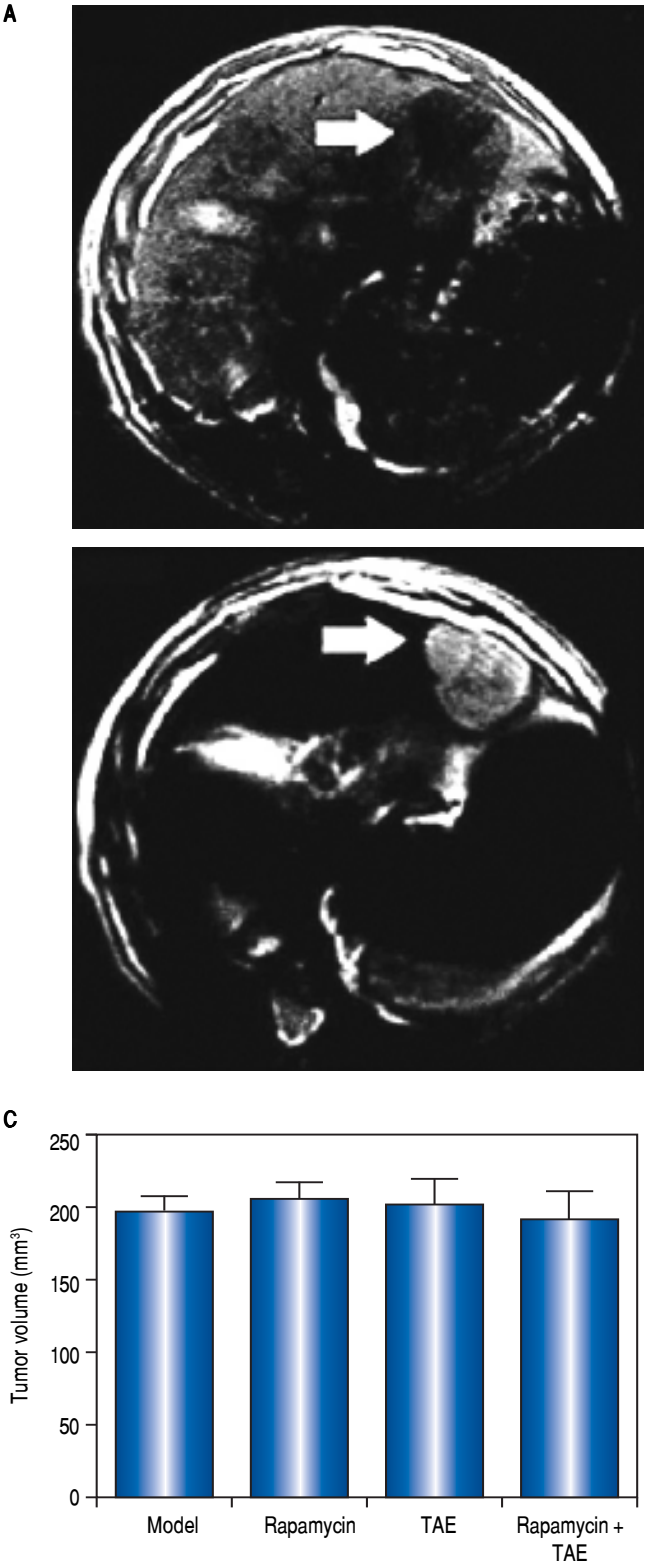

Figure 2. *The MRI examination on the 14th day after orthotopic hepatic transplantation and its tumor volume.* ***A.*** *T1WI showed low signal intensity of tumors.* ***B.*** *T2WI showed high signal intensity of tumors.* ***C.*** *The average volume of hepatic tumors of rats in each group.*

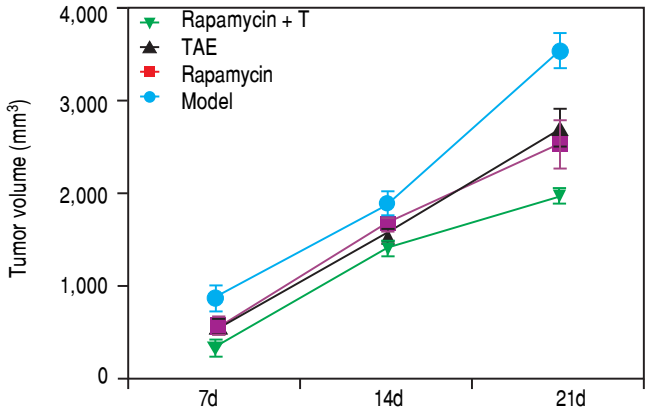

Figure 3. *Comparison of tumor volume of rats among different groups on the 7th, 14th and 21st day after treatment.*

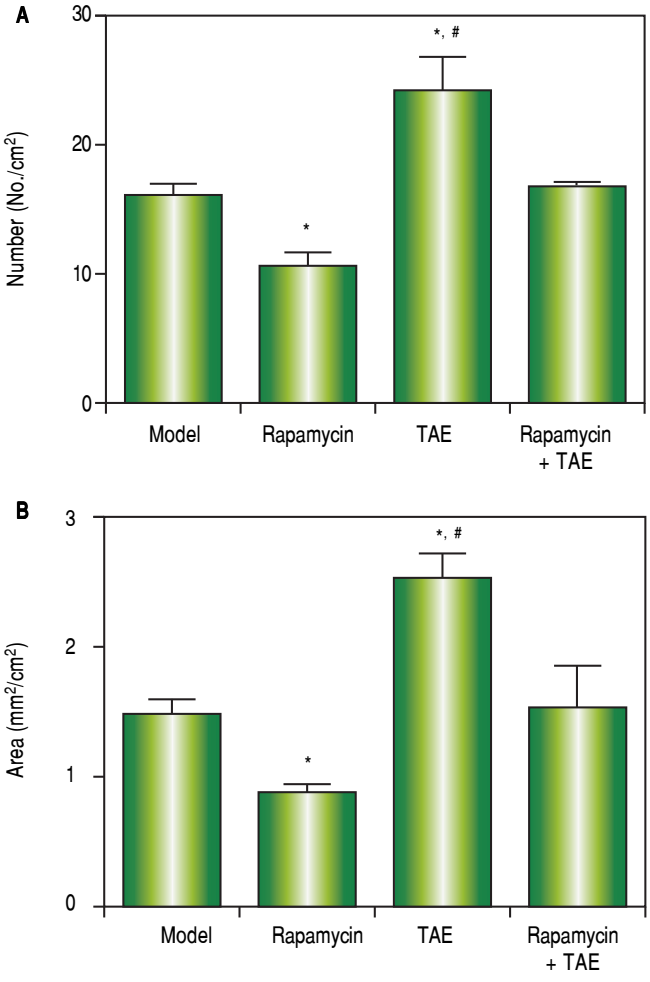

Figure 4. *Comparison of lung metastasis of rats among different groups on the 31st day after operation (2 weeks after treatment).* ***A.*** *Number of lung metastatic nodules.* ***B.*** *Size of metastatic nodules. * P < 0.05 compared with the Model group and the Rapamycin + TAE group. # P < 0.05 compared with the Rapamycin group.*

than those in the Model group and Rapamycin + TAE group (all $P < 0.05$). Additionally, no significant difference was found between the Model group and the Rapamycin + TAE group in these two indexes ($P > 0.05$) (Figure 4).

Effect of Rapamycin combined with TAE on the EMT and angiogenesis of HCC in rats

According to the qRT-PCR (Figure 5A), the hepatic tumor of rats in the TAE group were apparently up-regulated in the mRNA levels of mesenchymal markers (N-cadherin and Vimentin), but was dramatically lowered in the mRNA expression of the epithelial marker (E-cadherin) on the 31st day after operation (2 weeks after treatment), as compared with rats in the Model group (all $P < 0.05$). However, the situations of rats in the Rapamycin group were quite opposite to the TAE group, which could effectively inhibit the EMT process (all $P < 0.05$). In the meantime, rats in the Rapamycin + TAE group had no observable difference with those in the Model group regarding the EMT-related indexes (all $P > 0.05$). In addition, we further discovered the protein expressions of EMT-related molecules by Western blot and immunohistochemical staining in each group were in accordance with the trend of mRNA expression (Figure 5B-5D). Moreover, there was a significantly elevation in the expressions of HIF-1α and VEGF, as well as MVD-CD34 in the TAE group as revealed by immunohistochemical staining, when compared with the Model group, but were strikingly down-regulated after the combination treatment (all $P < 0.05$) (Figure 6).

Effects of Rapamycin combined with TAE on the survival of HCC rats

Kaplan-Meier Survival Curve demonstrated remarkable difference among different groups after treatment ($\chi^2 = 72.847$, $P < 0.001$, Figure 7). The median survival time of rats was 45.00 ± 1.581 days (Model), 62.00 ± 3.098 days (Rapamycin), 62.00 ± 0.516 days (TAE), and 70.00 ± 0.629 days (Rapamycin + TAE) respectively. Obviously, rats in the Rapamycin + TAE group had significantly longer survival time than the resting groups (all $P < 0.05$). Besides, the median survival time of rats in TAE and Rapamycin groups were apparently prolonged in comparison with that of the Model group (both $P < 0.05$).

DISCUSSION

One of the main results of this study demonstrated that both Rapamycin and TAE could obviously inhibit the growth of hepatic tumor and prolong the survival in rats with HCC, and more importantly, the combined use of

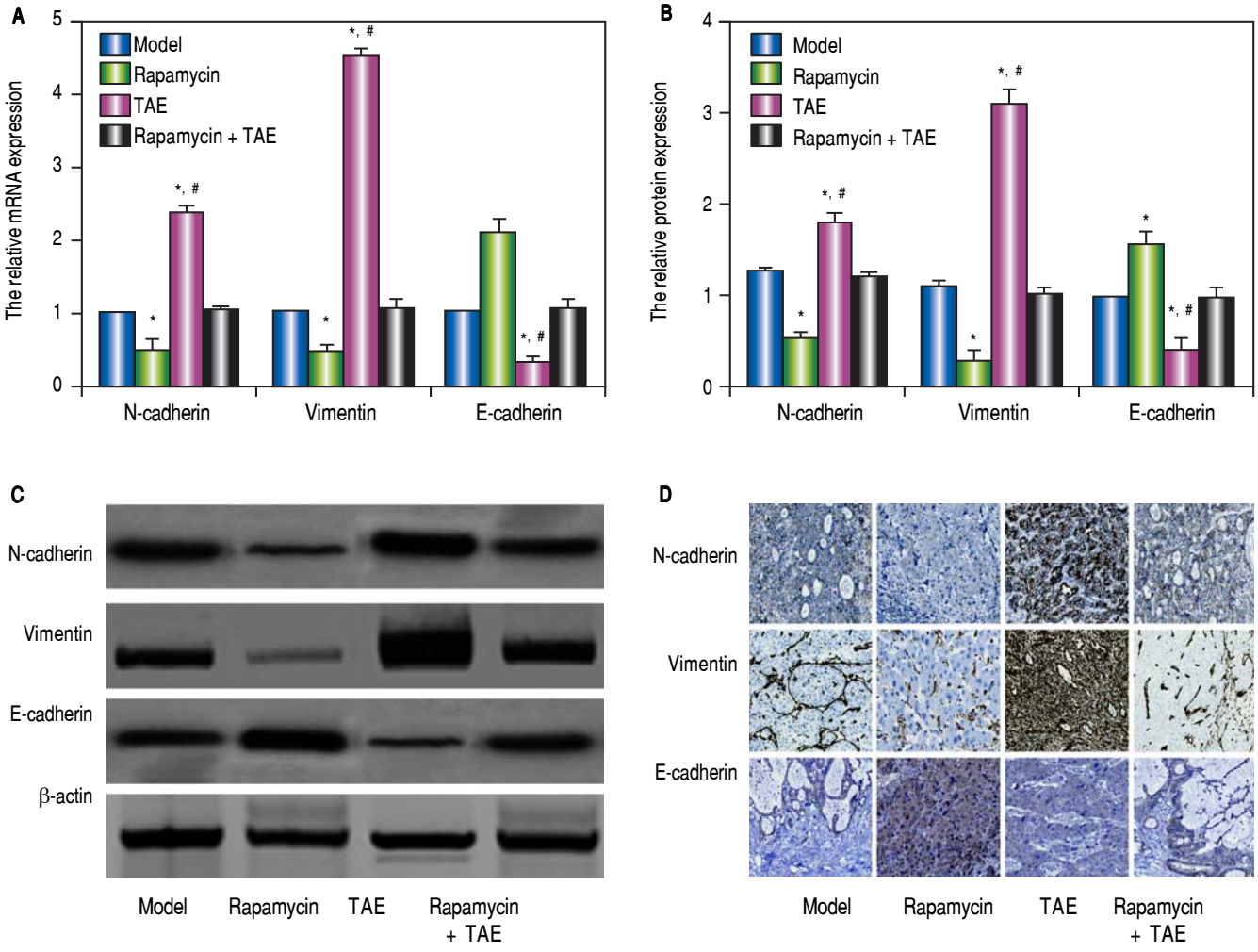

Figure 5. *Comparison of the expressions of EMT-related molecules in the hepatic tumor of rats in each group.* ***A.*** *The relative mRNA expression of N-cadherin, Vimentin and E-cadherin in hepatic tumor of rats detected by qRT-PCR.* ***B-C.*** *The protein expression of N-cadherin, Vimentin and E-cadherin in hepatic tumor of rats detected by Western blot.* ***D.*** *The protein expression of N-cadherin, Vimentin and E-cadherin hepatic tissues of rats detected by immunohistochemical staining. * P < 0.05 compared with the Model group and the Rapamycin + TAE group. # P < 0.05 compared with the Rapamycin group.*

Rapamycin with TAE would have better curative effects. As mTOR inhibitor, Rapamycin could effectively inhibit the presence of many diseases, including HCC. It was worthy to mention that Rapamycin, mediated by the immunophilin FKBP12, can form a Rapamycin-FKBP12 complex to lead to a mitotic block at the G1-S phase transition,[24] thereby further suppressing the phosphorylation of their downstream molecules P70S6K and 4EBP1 to inhibit the signal translation process,[25] and affecting the expression of anti-apoptotic protein c-IAP1 and pro-apoptotic protein BAD to result in the apoptosis of tumor cells.[26] In the study by Cifarelli V, *et al*., Rapamycin in combination with metformin can obviously decline pancreatic tumor growth and mTOR-related signaling via shared and distinct mechanisms.[27] Moreover, Neef M, *et al.* also reported Rapamycin as an effective anti-fibrotic drug, which can greatly attenuate disease progression and improve the survival in advanced cirrhosis.[28] Similarly, our study also showed apparently smaller tumor volume and prolonged survival in HCC rats after Rapamycin treatment. Meanwhile, TAE, currently recognized as an important micro-invasive modalities for the treatment of unresectable HCC, can selectively block the tumor blood supply and aggregate hypoxia and necrosis of tumor tissues, thus playing an effective role in the inhibition of tumor growth and the improvement of patients' survival.[29] Consistent with the results of previous studies, we observed that TAE treatment markedly suppress the tumor volume in rat with HCC. Notably, the hepatic tumor volume, as well as the median survival of rats with the combination therapy was apparently smaller than that with the Rapamycin alone and TAE alone, suggesting that TAE

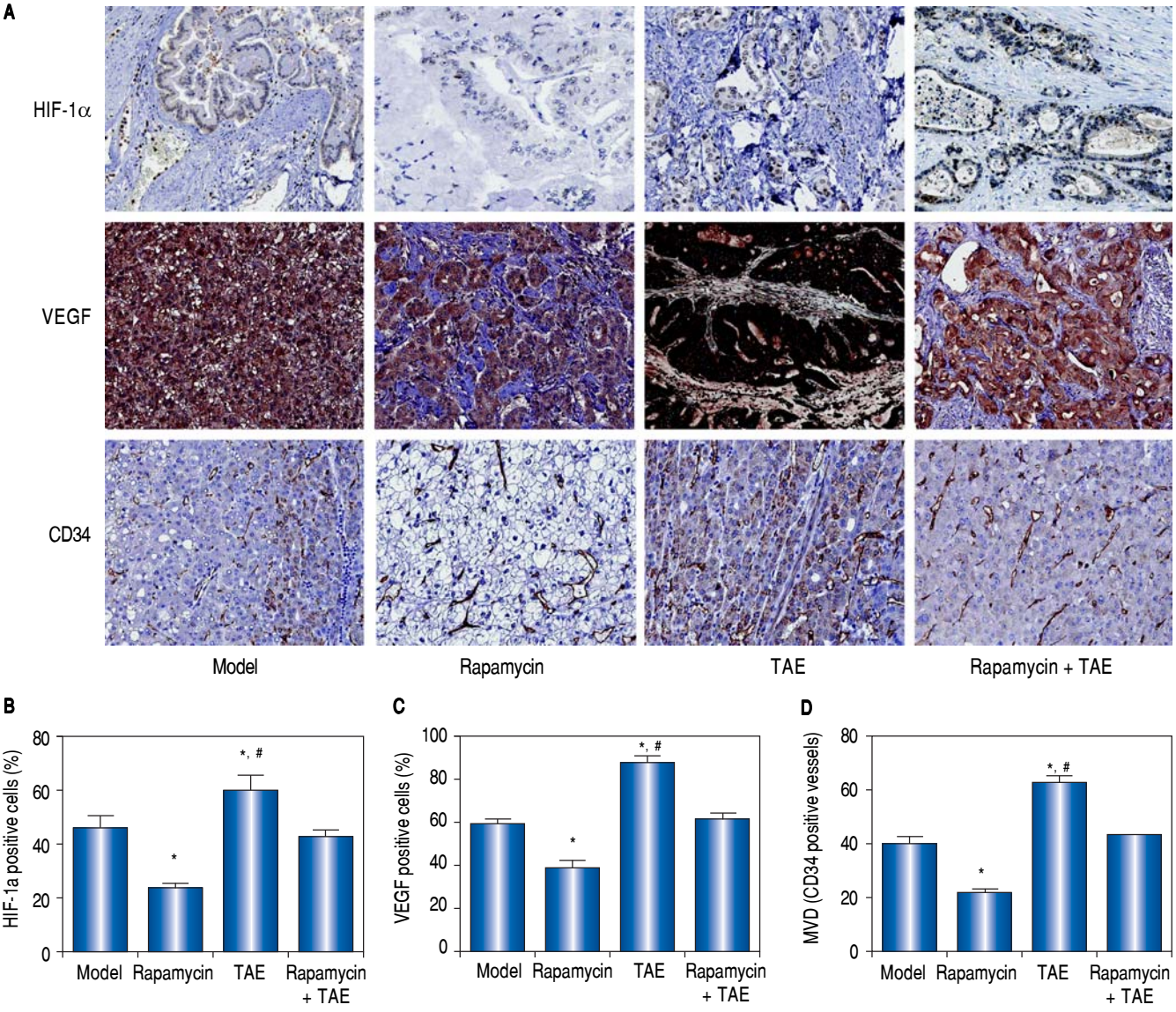

Figure 6. *Comparison of the expressions of HIF-1a and VEGF and the MVD-CD34 in hepatic tumor of rats in each group.* ***A.*** *The expressions of HIF-1a, VEGF and CD34 in hepatic tumor of rats in each group detected by immunohistochemical staining.* ***B-D.*** *The statistical graphs for the positive expression of HIF-1a* ***(B)****, VEGF* ***(C)*** *and CD34* ***(D)*** *in hepatic tumor of rats in each group. * P < 0.05 compared with the Model group and the Rapamycin + TAE group. # P < 0.05 compared with the Rapamycin group.*

combined with Rapamycin may become an effective method for the treatment of HCC.

Another important finding of this study showed the aggravated lung metastasis in HCC rats after TAE treatment, with the up-regulation of angiogenic factors including HIF-1 alpha and VEGF, and MVD-CD34. As we know, hypoxia is a very important post-operation feature of TAE for HCC.[6] Under hypoxic conditions, some HCC cells would induce the high expression of HIF-1α to regulate many downstream genes, such as VEGF, which are the potent regulatory factors in tumor angiogenesis, can promote the formation of new blood vessels to bring oxygen and nutrients to tumor cells for inducing the tumor invasion and metastasis.[30] As suggested by Rhee TK, *et al*., the levels of HIF-1α were greater in rabbit VX2 liver tumors after TAE.[31] Further, Dai F, *et al*. also discovered the obviously elevated expression of HIF-1α and VEGF, as well as increased level of MVD in the TAE-treated VX2 rabbit liver tumors, which was in agreement with our study,[6] indicating that hypoxia-induced tumor angiogenesis, possibly as the consequence of TAE, might be accepted as a marker of tumor development and metastasis. On the other hand,

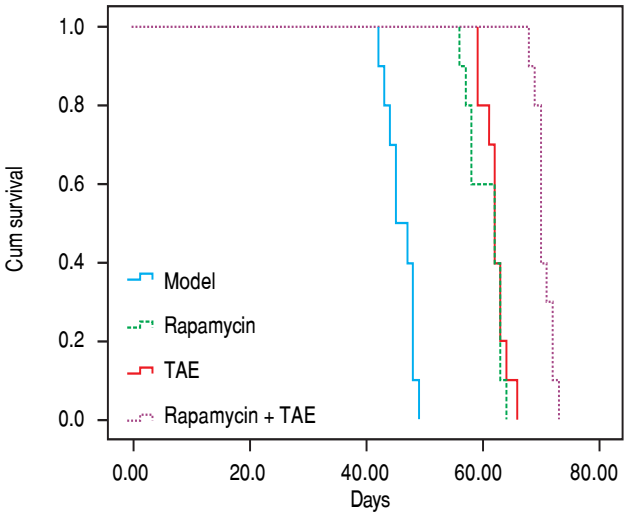

Figure 7. *Effects of Rapamycin combined with TAE on the survival of HCC rats.*

evidence supported that hypoxia can also promote angiogenesis via the induction of EMT formation,[32] with the down-regulation of epithelial markers and the upregulation of mesenchymal markers, ultimately playing roles in tumor invasion and metastasis.[33] Therefore, our study detected the EMT-related molecules at the levels of both mRNA and protein in rats with HCC and demonstrated an elevation of N-cadherin and Vimentin and a reduction of E-cadherin after TAE treatment, which was in line with the results provided by ZT Fang.[34] Besides, Rapamycin can greatly restore the expression of E-cadherin to inhibit EMT of proximal tubular epithelial cells and exerted a protective function on EMT process through the inhibition of the Rho GTPases.[35] Coincidentally, in our study, after the combination treatment with Rapamycin and TAE, the expression of N-cadherin and Vimentin was notably reduced in HCC tissues, while the expression of E-cadherin was obviously elevated, and the lung metastasis, EMT formation, and the angiogenesis have been greatly alleviated. Additionally, a previous study discovered the existence of molecular crosstalk between the mTOR signaling pathway and the VM signaling pathway.[36] Not surprisingly, our study also demonstrated the significant reduction of VEGF and MVD-CD34 expression in HCC after Rapamycin combined with TAE, which was further verified by Huang M, *et al.* in gliomas.[37]

To sum up, Rapamycin combined with TAE may effectively enhance the inhibition of tumor growth, lung metastasis, as well as the EMT formation and tumor angiogenesis of HCC, providing a new approach for the treatment of HCC recurrence and metastasis. In the future studies, we will conduct some vitro experiments to verify our findings and further explore the relative mechanisms.

ACKNOWLEDGMENTS

We would like to give our sincere appreciation to the reviewers for their helpful comments on this paper.

CONFLICTS OF INTEREST

The authors have no conflict of interest.

REFERENCES

1. Tang B, Tang F, Wang Z, Qi G, Liang X, Li B, Yuan S, et al. Upregulation of Akt/NF-kappaB-regulated inflammation and Akt/Bad-related apoptosis signaling pathway involved in hepatic carcinoma process: suppression by carnosic acid nanoparticle. *Int J Nanomedicine* 2016; 11: 6401-20. 10.2147/IJN.S101285
2. Liu L, Zhao Y, Jia J, Chen H, Bai W, Yang M, Yin Z, et al. The Prognostic Value of Alpha-Fetoprotein Response for Advanced-Stage Hepatocellular Carcinoma Treated with Sorafenib Combined with Transarterial Chemoembolization. *Sci Rep* 2016; 6: 19851. 10.1038/srep19851
3. Goseki N, Nosaka T, Endo M, Koike M. Nourishment of hepatocellular carcinoma cells through the portal blood flow with and without transcatheter arterial embolization. *Cancer* 1995; 76: 736-42.
4. Taniguchi K, Nakata K, Kato Y, Sato Y, Hamasaki K, Tsuruta S, Nagataki S. Treatment of hepatocellular carcinoma with transcatheter arterial embolization. Analysis of prognostic factors. *Cancer* 1994; 73: 1341-5.
5. Acunas B, Rozanes I. Hepatocellular carcinoma: treatment with transcatheter arterial chemoembolization. *Eur J Radiol* 1999; 32: 86-9.
6. Dai F, Zhang X, Shen W, Chen J, Liu L, Gao G. Liposomal curcumin inhibits hypoxia-induced angiogenesis after transcatheter arterial embolization in VX2 rabbit liver tumors. *Onco Targets Ther* 2015; 8: 2601-11. 10.2147/OTT.S87931
7. Zhao H, Ahirwar DK, Oghumu S, Wilkie T, Powell CA, Nasser MW, Satoskar AR, et al. Endothelial Robo4 suppresses breast cancer growth and metastasis through regulation of tumor angiogenesis. *Mol Oncol* 2016; 10: 272-81. 10.1016/j.molonc.2015.10.007
8. Nitta-Seko A, Nitta N, Sonoda A, Otani H, Tsuchiya K, Ohta S, Takahashi M, et al. Anti-tumour effects of transcatheter arterial embolisation administered in combination with thalidomide in a rabbit VX2 liver tumour model. *Br J Radiol* 2011; 84: 179-83. 10.1259/bjr/53771502
9. Wei K, Wang M, Zhang W, Mu H, Song TQ. Neutrophil-lymphocyte ratio as a predictor of outcomes for patients with hepatocellular carcinoma undergoing TAE combined with Sorafenib. *Med Oncol* 2014; 31: 969. 10.1007/s12032-014-0969-5
10. Wang C, Yu JT, Miao D, Wu ZC, Tan MS, Tan L. Targeting the mTOR signaling network for Alzheimer's disease therapy. *Mol Neurobiol* 2014; 49: 120-35. 10.1007/s12035-013-8505-8
11. Liu F, Zhang W, Yang F, Feng T, Zhou M, Yu Y, Yu X, et al. Interleukin-6-stimulated progranulin expression contributes to the malignancy of hepatocellular carcinoma cells by activating mTOR signaling. *Sci Rep* 2016; 6: 21260. 10.1038/srep21260
12. Mabuchi S, Kuroda H, Takahashi R, Sasano T. The PI3K/AKT/mTOR pathway as a therapeutic target in ovarian cancer.

Gynecol Oncol 2015; 137: 173-9. 10.1016/j.ygyno.2015.02.003
13. Zhao Q, Wang Z, Wang Z, Wu L, Zhang W. Aspirin may inhibit angiogenesis and induce autophagy by inhibiting mTOR signaling pathway in murine hepatocarcinoma and sarcoma models. *Oncol Lett* 2016; 12: 2804-10. 10.3892/ol.2016.5017
14. Xue ZG, Niu PG, Shi DH, Liu Y, Deng J, Chen YY. Cardamonin Inhibits Angiogenesis by mTOR Downregulation in SKOV3 Cells. *Planta Med* 2016; 82: 70-5. 10.1055/s-0035-1557901
15. Huo Y, Iadevaia V, Proud CG. Differing effects of rapamycin and mTOR kinase inhibitors on protein synthesis. *Biochem Soc Trans* 2011; 39: 446-50. 10.1042/BST0390446
16. Guba M, von Breitenbuch P, Steinbauer M, Koehl G, Flegel S, Hornung M, Bruns CJ, et al. Rapamycin inhibits primary and metastatic tumor growth by antiangiogenesis: involvement of vascular endothelial growth factor. *Nat Med* 2002; 8: 128-35. 10.1038/nm0202-128
17. Sekiguchi Y, Zhang J, Patterson S, Liu L, Hamada C, Tomino Y, Margetts PJ. Rapamycin inhibits transforming growth factor beta-induced peritoneal angiogenesis by blocking the secondary hypoxic response. *J Cell Mol Med* 2012; 16: 1934-45. 10.1111/j.1582-4934.2011.01493.x
18. Xie J, Wang X, Proud CG. mTOR inhibitors in cancer therapy. F1000Res. 2016; 5:10.12688/f1000research.9207.1
19. Yuan R, Kay A, Berg WJ, Lebwohl D. Targeting tumorigenesis: development and use of mTOR inhibitors in cancer therapy. *J Hematol Oncol* 2009; 2: 45. 10.1186/1756-8722-2-45
20. Owonikoko TK. Inhibitors of mTOR pathway for cancer therapy, moving on from rapalogs to TORKinibs. *Cancer* 2015; 121: 3390-2. 10.1002/cncr.29424
21. Orlans FB. Ethical decision making about animal experiments. *Ethics Behav* 1997; 7: 163-71. 10.1207/s15327019eb0702_7
22. Futakuchi M, Hirose M, Ogiso T, Kato K, Sano M, Ogawa K, Shirai T. Establishment of an in vivo highly metastatic rat hepatocellular carcinoma model. *Jpn J Cancer Res* 1999; 90: 1196-202.
23. Zhang Q, Chen X, Zhou J, Zhang L, Zhao Q, Chen G, Xu J, et al. CD147, MMP-2, MMP-9 and MVD-CD34 are significant predictors of recurrence after liver transplantation in hepatocellular carcinoma patients. *Cancer Biol Ther* 2006; 5: 808-14.
24. Rossi A, Pica-Mattoccia L, Cioli D, Klinkert MQ. Rapamycin insensitivity in Schistosoma mansoni is not due to FKBP12 functionality. *Mol Biochem Parasitol* 2002; 125: 1-9.
25. Fuentes EN, Einarsdottir IE, Paredes R, Hidalgo C, Valdes JA, Bjornsson BT, Molina A. The TORC1/P70S6K and TORC1/4EBP1 signaling pathways have a stronger contribution on skeletal muscle growth than MAPK/ERK in an early vertebrate: Differential involvement of the IGF system and atrogenes. *Gen Comp Endocrinol* 2015; 210: 96-106. 10.1016/j.ygcen.2014.10.012
26. Song X, Dilly AK, Kim SY, Choudry HA, Lee YJ. Rapamycin-enhanced mitomycin C-induced apoptotic death is mediated through the S6K1-Bad-Bak pathway in peritoneal carcinomatosis. *Cell Death Dis* 2014; 5:e1281. 10.1038/cddis.2014.242
27. Cifarelli V, Lashinger LM, Devlin KL, Dunlap SM, Huang J, Kaaks R, Pollak MN, et al. Metformin and Rapamycin Reduce Pancreatic Cancer Growth in Obese Prediabetic Mice by Distinct MicroRNA-Regulated Mechanisms. *Diabetes* 2015; 64: 1632-42. 10.2337/db14-1132
28. Neef M, Ledermann M, Saegesser H, Schneider V, Reichen J. Low-dose oral rapamycin treatment reduces fibrogenesis, improves liver function, and prolongs survival in rats with established liver cirrhosis. *J Hepatol* 2006; 45: 786-96. 10.1016/j.jhep.2006.07.030
29. Willatt JM, Francis IR, Novelli PM, Vellody R, Pandya A, Krishnamurthy VN. Interventional therapies for hepatocellular carcinoma. *Cancer Imaging* 2012; 12: 79-88. 10.1102/1470-7330.2012.0011
30. Liu K, Min XL, Peng J, Yang K, Yang L, Zhang XM. The Changes of HIF-1alpha and VEGF Expression After TACE in Patients With Hepatocellular Carcinoma. *J Clin Med Res* 2016; 8: 297-302. 10.14740/jocmr2496w
31. Rhee TK, Young JY, Larson AC, Haines GK, 3rd, Sato KT, Salem R, Mulcahy MF, et al. Effect of transcatheter arterial embolization on levels of hypoxia-inducible factor-1alpha in rabbit VX2 liver tumors. *J Vasc Interv Radiol* 2007; 18: 639-45. 10.1016/j.jvir.2007.02.031
32. Li W, Zong S, Shi Q, Li H, Xu J, Hou F. Hypoxia-induced vasculogenic mimicry formation in human colorectal cancer cells: Involvement of HIF-1a, Claudin-4, and E-cadherin and Vimentin. *Sci Rep* 2016; 6: 37534. 10.1038/srep37534
33. Ye Z, Zhou M, Tian B, Wu B, Li J. Expression of lncRNA-CCAT1, E-cadherin and N-cadherin in colorectal cancer and its clinical significance. *Int J Clin Exp Med* 2015; 8: 3707-15.
34. Fang ZT, Wang GZ, Zhang W, Qu XD, Liu R, Qian S, Zhu L, et al. Transcatheter arterial embolization promotes liver tumor metastasis by increasing the population of circulating tumor cells. *Onco Targets Ther* 2013; 6: 1563-72. 10.2147/OTT.S52973
35. Xiang S, Li M, Xie X, Xie Z, Zhou Q, Tian Y, Lin W, et al. Rapamycin inhibits epithelial-to-mesenchymal transition of peritoneal mesothelium cells through regulation of Rho GTPases. *FEBS J* 2016; 283: 2309-25. 10.1111/febs.13740
36. Tang J, Wang J, Fan L, Li X, Liu N, Luo W, Wang J, et al. cRGD inhibits vasculogenic mimicry formation by down-regulating uPA expression and reducing EMT in ovarian cancer. *Oncotarget* 2016; 7: 24050-62. 10.18632/oncotarget.8079
37. Huang M, Ke Y, Sun X, Yu L, Yang Z, Zhang Y, Du M, et al. Mammalian target of rapamycin signaling is involved in the vasculogenic mimicry of glioma via hypoxia-inducible factor-1alpha. *Oncol Rep* 2014; 32: 1973-80. 10.3892/or.2014.3454

Correspondence and reprint request:
You-Ying Feng, M.D, Ph.D.
The First People's Hospital of Jingzhou, No. 8, Hangkong Road, Shashi District, Jingzhou 434000, Hubei, P.R.China.
Tel.: 0716-8125931
E-mail: fengyy1719@sina.com